Biogeosciences Discuss., https://doi.org/10.5194/bg-2018-117
Manuscript under review for journal Biogeosciences
Discussion started: 7 March 2018

Biogeosciences Discussions Open Access EGU

A model of mercury cycling and isotopic fractionation in the ocean

David E. Archer[1], Joel D. Blum[2]

[1]Department of the Geophysical Sciences, University of Chicago, Chicago, 60637, USA
[2]Department of Earth and Environmental Sciences, University of Michigan, Ann Arbor, Michigan 48109

Correspondence to: David E. Archer (d-archer@uchicago.edu)

Abstract. Mercury speciation and isotopic fractionation processes have been incorporated into the HAMOCC offline ocean tracer advection code. The model is fast enough to allow a wide exploration of the sensitivity of the Hg cycle in the oceans, and of human exposure to Hg via monomethyl-Hg incorporation into fish. Vertical particle transport of Hg appears to play a discernable role in setting present-day Hg distributions, which we surmise by the fact that in simulations without particle transport, the high present-day Hg deposition rate leads to an Hg maximum at the sea surface, rather than a subsurface maximum as observed. Hg particle transport has only a relatively small impact on anthropogenic Hg uptake, but it sequesters Hg deeper in the water column, so that excess Hg is retained in the model ocean for longer after anthropogenic Hg deposition is stopped. The concentration of monomethyl Hg is sensitive to its production rate, with model experiments suggesting that human impacts on ocean oxygen concentrations could have as significant an impact on oceanic MMHg concentration as the anthropogenic Hg emission itself. Eight different isotopic fractionation mechanisms are simulated, independently and combined together, to predict their expression in the spatial distributions of isotopic signatures of Hg species in the ocean.

1 Background

The element mercury, Hg, is fundamentally toxic to our metabolic chemistry, and has no known use or function in metabolism (Clarkson and Magos, 2006). It is the only heavy metal known to magnify its toxicity by bio-accumulating up the food chain, and the main human exposure to Hg is via seafood which accumulates Hg from the ocean (Chen et al., 2016;Schartup et al., 2018). Humans have been mining and mobilizing Hg into the Earth surface environment for thousands of years, as by-product of coal combustion, and for its use in gold mining and in products such as electronics and light bulbs (Amos et al., 2013;Driscoll et al., 2013;Krabbenhoft and Sunderland, 2013;Lamborg et al., 2014;Obrist et al., 2018;Streets et al., 2017;Mason et al., 2012). The Hg load in the surface ocean has increased by a factor of 3-5; a massive human impact on the global Hg cycle (Streets et al., 2017).

Hg can be extremely mobile in the environment, with long-lived forms in the gas phase in the atmosphere, and with soluble phases allowing it to travel through soils and into the oceans (Fitzgerald et al., 2007). The soft electronic Hg atom has a high affinity for complexing or adsorbing onto sulfur-rich ligands in organic matter (Schartup et al., 2015), that leads Hg to

accumulate in organic carbon in soils (Amos et al., 2013;Smith-Downey et al., 2010;Biswas et al., 2008) and sediments (Hollweg et al., 2010). The high mobility of Hg implies that these deposits are transient even in the steady-state pre-human Hg cycle (Amos et al., 2013), and that they can be potentially mobilized by human impacts such as the thawing of Arctic permafrost (Schuster et al., 2018).

The Hg cycle is analogous to the carbon cycle, in which material mined from the solid Earth is released to a fast surface system consisting of soils and oceans in communication via the atmosphere. In both cases, the long-term sink for the perturbation is burial in sediments of the ocean. Because these burial fluxes are relatively slow, it will take a long time for the perturbation to subside: thousands of years for the Hg cycle (Amos et al., 2013), and hundreds of thousands of years for carbon (Archer et al., 2009). Other forms of environmental degradation that will persist for thousands of years include actinide radioactive waste, and some anthropogenic gases such as sulfur hexafluoride (Ray et al., 2017).

It is extremely challenging to predict the future of human exposure to Hg, because the Hg cycle is so rich and complex (Blum, 2013). One challenge has been to characterize the quantitative role of Hg adsorbed onto sinking particles in the ocean (Lamborg et al., 2016), which will determine how deeply anthropogenic Hg may have penetrated into the ocean (Lamborg et al., 2014;Munson et al., 2015;Zhang et al., 2014). Another is to understand the factors that control the production of methyl mercury, which is the bio-accumulating form but which comprises only a small fraction of the Hg in the ocean (Schartup et al., 2015;Schartup et al., 2013;Ortiz et al., 2015;Lehnherr et al., 2011;Lehnherr, 2014;Jonsson et al., 2016;Chakraborty et al., 2016;Blum et al., 2013).

Stable isotopes provide a powerful tool for determining the origins ((Kwon et al., 2014;Li et al., 2014;Sherman et al., 2015;Sherman et al., 2013;Balogh et al., 2015;Demers et al., 2015;Donovan et al., 2014) and transformations (Kwon et al., 2013;Kwon et al., 2014) of Hg in the natural environment. Hg has seven stable isotopes with six at high abundance (<1%). Most chemical processes fractionate the various isotopes strictly according to their mass differences (called Mass Dependent Fractionation or MDF). If all fractionation processes were strictly mass dependent, measurements of the proportions of more than two isotopes would be redundant information. However, the complex electronic structure of the Hg atom makes it susceptible to light-stimulated redox reactions, reduction of Hg(2+) or MMHg, that exhibit Mass Independent Fractionation (MIF), which distinguishes between isotopes beyond their mass differences (Blum et al., 2014;Bergquist and Blum, 2009). Odd mass number mass independent fractionations, or (odd-MIF), are produced by two mechanisms. Large magnitude effects are seen in kinetic short-lived radical pair reactions and are caused by the magnetic isotope effect. Smaller magnitude even-MIF can also be produced during dark equilibrium reduction and oxidation reactions by the nuclear volume effect. But the large magnitude (>~0.4‰) odd MIF is only from photochemical processes. Even-MIF has only been observed in atmospheric samples and is believed to occur in the tropopause by an as-yet unidentified mechanism. Mass independent fractionations provide multiple degrees of freedom, allowing measurements of the proportions of all the isotopes to carry much more information than would be possible in a strictly MDF world.

We have incorporated a model of the chemical transformations and isotopic fractionations of Hg in the ocean into the Hamocc offline ocean passive tracer advection model (Maier-Reimer and Hasselmann, 1987). The flow field is taken from

Biogeosciences Discuss., https://doi.org/10.5194/bg-2018-117
Manuscript under review for journal Biogeosciences
Discussion started: 7 March 2018

the Large Scale Geostrophic (LSG) dynamics model, which is also extremely fast and efficient for 3-D ocean flow (Maierreimer et al., 1993). The LSG physical model takes a time step of a month by eliminating non-geostrophic parts of the circulation that would be violated by this extremely long time step. The HAMOCC tracer advection model takes an annual average flow field from 12 monthly time steps of the LSG model and uses it to advect tracers through the ocean. While the tracers are flowing, they exchange with the atmosphere (in the case of CO_2 and O_2), and with biology (as CO_2 and O_2, alkalinity, and nutrients).

The distribution of Hg in the ocean today is the product of a presumably steady state natural Hg cycle, which takes thousands of years to achieve in the model due to the ocean turnover time, followed by an extreme human perturbation lasting thousands of years (and which could persist for thousands of years into the future). HAMOCC is probably still the fastest off-line 3-D ocean tracer advection code in existence, ideal for studying the sensitivity of the ocean Hg cycle on these long time scales. This paper is also the first attempt to our knowledge to simulate the isotopic fractionation processes of Hg in the ocean, which take thousands of years to express themselves globally.

2 Modeling Methods

2.1 Mercury Geochemistry Solvers

The geochemical cycling of Hg in the ocean in Hg-HAMOCC is similar in conception to previous models (Semeniuk and Dastoor, 2017;Zhang et al., 2014) (but with modifications as described in Results section) (Figure 1). Hg interconverts between Hg(2+), Hg(0) metal, mono-methyl Hg (MMHg), di-methyl Hg (DMHg), and Hg adsorbed to sinking particles (Hg-P). The rates of the dark reactions are correlated to each other and to the overall rate of metabolic activity in the (Semeniuk and Dastoor, 2017) model and ours, with the scaling factors as shown in Figure 1. The rate constant for MMHg production from Hg(2+) is proportional to the rate of POC degradation, which is derived from the attenuation with depth of the sinking POC flux in HAMOCC (expressed as a volumetric rate of POC degradation). Other Hg transformation reactions are provoked by light, and only take place near the surface ocean (Blum et al., 2014;Bergquist and Blum, 2007). The rate of photochemical reactions in Hg-HAMOCC is more intense at low latitude, using the latitudinal function that governs export production rates in HAMOCC which provides about a factor of two difference between low and high latitudes. The photochemical reaction rates are attenuated with water depth, using an e-folding depth scale of 50 meters. The wavelength dependence of photochemical reactions and fractionations is complex (Rose et al., 2015), and the attenuation depth of the light varies with frequency, so the 50m depth scale is only an approximation.

The rates of gas evasion of Hg(0) and DMHg are taken to be proportional to the concentrations of the species, on the assumption that atmospheric concentrations are negligible. The Hg system in the surface ocean is driven by deposition influx of Hg(2+), which is applied at a uniform rate around the world.

All of the rate constants in Hg-HAMOCC are first-order, which is to say that the chemical rates are determined by multiplying the rate constant by a single species concentration to the first power. Rates of conversion between these species

Biogeosciences Discuss., https://doi.org/10.5194/bg-2018-117
Manuscript under review for journal Biogeosciences
Discussion started: 7 March 2018

are generally fast, some much faster than the 1-year time step of the tracer code. For this reason, solvers were written to find steady state distributions of the Hg species. Because the Hg system is strongly driven at the sea surface by air-sea fluxes, a separate solver system was developed for surface grid points than the one applied to subsurface grid points.

Export of sinking Hg-P is done separately from the speciation calculations in subsurface waters, but simultaneously with the speciation calculations in the surface ocean. Hg advection by ocean circulation is also done in an independent step from the chemistry and particle components. Since the Hg speciation is imposed to be at equilibrium by the speciation solvers, there is no need to carry speciation information through the advective system, which only has to carry around a single tracer for the total Hg concentration. To treat the isotopic systematics of the Hg cycle, we added two additional advected tracers, for total ^{199}Hg and ^{202}Hg concentrations. Mass dependent fractionation processes are imposed on both ^{202}Hg and ^{199}Hg systems, with a factor of 3.96 scaling reflecting the differences to mass 198. Mass independent fractionation in photochemical reduction of Hg(2+) and MMHg is imposed only on the ^{199}Hg system (isotopic systematics are described more fully below).

2.1.1 Surface ocean chemistry solver

For the surface ocean, the distribution of Hg among the dissolved species is determined by a balance of Hg fluxes through the system: rain input of Hg(2+), and removal by Hg(2+) scavenging on sinking particles and degassing as Hg(0) and DMHg. Since Hg degassing and sinking rates are linearly related to dissolved species concentrations (assuming an atmospheric concentration of 0), the Hg concentrations, in the steady state, are able to find values at which the incoming and loss fluxes balance. The equations are

$$\begin{bmatrix} -k_{20}-k_{2M}-k_{2D}-S & k_{02} & 0 & 0 \\ k_{20} & -k_{evp} & k_{M0} & 0 \\ k_{2M} & 0 & -k_{M0}-k_{MD} & k_{DM} \\ k_{2D} & 0 & k_{MD} & -k_{evp}-k_{DM} \end{bmatrix} \begin{bmatrix} [Hg(2+)] \\ [Hg(0)] \\ [MMHg] \\ [DMHg] \end{bmatrix} = \begin{bmatrix} -Rain_{Hg(2+)} \\ 0 \\ 0 \\ 0 \end{bmatrix}$$

where k denotes a first-order rate constant, subscripts denote reactant then product where 2 = Hg(2+), 0 = Hg(0), D = DMHg, and M = MMHg. The subscript evp stands for evaporation, and S is a rate constant for Hg(2+) sinking on particles

$$S = \left(1 - \frac{1}{k_b[POC]+1}\right)\frac{R}{dz}$$

comprised of the POC concentration, the scavenging constant, and the assumed POC sinking velocity R. The diagonal terms in the first matrix represent sinks of the chemical species listed in the second matrix, when those sinks are calculated as the rate constants in the diagonal multiplied by the species concentration (which is solved for). The positive off-diagonal terms in the first matrix represent sources of species, which are calculated as rate constants times the concentration of the origin species. Nonzero terms in the right-hand matrix represent fixed-rate sources, of which deposition of Hg(2+) is the only

Biogeosciences Discuss., https://doi.org/10.5194/bg-2018-117
Manuscript under review for journal Biogeosciences
Discussion started: 7 March 2018

example. This linear algebraic calculation solves for the steady-state concentrations of the four Hg species without iteration (in contrast to an analogous solver in HAMOCC for CO2 system chemistry).

2.1.2 Subsurface ocean chemistry solver

The Hg cycle in the deep ocean differs from that of the surface in that fluxes of Hg into and out of the system (by desorption of Hg(2+) from particles) are slow relative to the rates of interconversion between the Hg species. Because all of the rate constants are first-order, the relative proportions of the species are independent of the total Hg concentration. The solver finds steady state values of all species relative to that of Hg2+, then scales everything to fit the total Hg concentration as produced by the advection routine. The equations are

$$\begin{bmatrix} -k_{02} & k_{M2} & 0 \\ 0 & -k_{M0} & k_{DM} \\ 0 & k_{MD} & -k_{DM} \end{bmatrix} \begin{bmatrix} [Hg(0)] \\ [MMHg] \\ [DMHg] \end{bmatrix} = \begin{bmatrix} 0 \\ 1pM \times k_{Hg(2+)} \\ 0 \end{bmatrix}$$

where a concentration of 1pM is assumed for [Hg(2+)], in order to work out the relative proportions of the other species. After the proportions of all the species concentrations are worked out, they are scaled to match the total Hg concentration as it is slowly changed by advection and desorption from POC. Profiles of the Hg species, in the Atlantic and Pacific, are shown in Figure 2. The locations are chosen to span the range of variability in the model, from highly productive equatorial Pacific to the oligotrophic Atlantic.

2.2 Hg adsorption and transport on particles

The human biological impacts of Hg occur because of the chemical affinity of Hg for organic matter, in particular to organic sulfur ligands. The same chemistry leads Hg to adsorb onto organic matter in the ocean, leading to a vertical sinking flux of adsorbed Hg on particles (Lamborg et al., 2016). Characterizing this flux is complicated by the fact that sinking particles compete for Hg with suspended and dissolved organic carbon (Han et al., 2006;Fitzgerald et al., 2007).

The biological pump in HAMOCC is represented as an instantaneous vertical redistribution of nutrients and other associated biological elements, without ever resolving them into particles or tracking their sinking. We constructed a hypothetical POC profile from this functioning of HAMOCC by choosing a sinking velocity that would transform the export production from the euphotic zone in Hamocc into surface POC concentrations that are close to the observed mean concentration of about 5 micromolar. This sinking velocity of 2 meters per day is much slower than the actual inferred sinking velocities of the particles that carry the bulk of the material caught in sediment traps, of about 100 meters per day, but it is similar to that used by (Semeniuk and Dastoor, 2017;Lamborg et al., 2016), and comparable to the result of modeling thorium on particles (Anderson et al., 2016).

Biogeosciences Discuss., https://doi.org/10.5194/bg-2018-117
Manuscript under review for journal Biogeosciences
Discussion started: 7 March 2018

A second degree of freedom in the system of sinking Hg particles is the adsorption constant K_d, defined as [Hg-P] / [Hg(2+)], values of which vary by orders of magnitude in the literature. Semeniuk (2017) used a value of $2 \cdot 10^5$, while Lamborg (2016) derived a value of about $4 \cdot 10^6$, a factor of 20 higher. The preferred value of K_d in our formulation is $1 \cdot 10^4$, which is 20 times lower than the Semeniuk (2017) value. The target of our tuning of K_d was to reproduce the salient result from the model of Semeniuk (2017) and the data from Lamborg (2016) that about 5% of the Hg(2+) in surface waters is bound to sinking particles (Figure 3). The huge differences must arise due to differences in the assumed concentration of POC in the different formulations. Figure 4 is a map of the bound fraction in surface waters, showing considerable spatial variation due to differences in [POC], and showing the locations of the profiles in Figure 3.

For Hg sinking, after tuning the K_d to get the bound fraction right, a sinking velocity of about 400 meters / year is required to reproduce the Hg sinking flux to the sea floor in steady state from Semeniuk (2017) (Figure 5). However, sinking fluxes of Hg in the mid water column are about a factor of three lower than equatorial and North Pacific sediment trap fluxes from Munson (2015), so the models could be underpredicting the real particles fluxes if the Munson (2015) data are globally representative.

The turnover time of dissolved Hg, with respect to transiting through the water column on sinking particles, depends on the sinking velocity, as shown in Figure 6. Values approaching 1000 years in the deep ocean have been reported in other models (Semeniuk and Dastoor, 2017;Zhang et al., 2014), and imply that circulation plays a major role in determining deep ocean Hg concentrations.

2.3 Isotopic fractionation

Potential isotopic fractionations associated with any of the processes in the Hg cycle are treated as kinetic effects: slight perturbations in the rates of chemical transformations (rather than at equilibrium). This allows Hg-HAMOCC to impose fractionation effects onto the kinetic expressions in the solvers for surface and subsurface Hg speciation. The altered kinetics are applied to alternative Hg concentration fields styled after even and odd isotopes of Hg, specifically, ^{199}Hg and ^{202}Hg. The MIF fractionation only applies to odd ^{199}Hg, whereas MDF processes apply to both isotopes, with an impact roughly 4 times stronger for mass 202 than for 199 (relative to 198). As for isotopic measurements in reality, the MIF component of the fractionation is isolated by subtracting from the measured d199 value the expected MDF based on the δ^{202} value, to produce a composite quantity Δ^{199}. As was done by Ernst Maier-Reimer in HAMOCC many years ago (Maier-Reimer, 1984), it is helpful in the model to set the nominal computational concentrations of the three isotopes equal, rather than at some artibrary ratio as in nature, to minimize computational rounding errors. The delta values are insensitive to this convenience, because the nominal ratio is subtracted out to calculate delta values. The solver finds the impact of the fractionation on the steady-state isotopic signatures in the Hg system: the expression of the isotope effects within the kinetic ocean Hg cycle.

Biogeosciences Discuss., https://doi.org/10.5194/bg-2018-117
Manuscript under review for journal Biogeosciences
Discussion started: 7 March 2018

2.4 The Anthropogenic Perturbation

Human activity has resulted in increased Hg emission to the biosphere for centuries (Streets et al., 2011;Streets et al., 2017;Amos et al., 2013;Horowitz et al., 2014), which has lead to an increase in Hg deposition to the ocean. Because of the tendency of Hg to recycle in the environment, the relationship between emissions and deposition is not simple and immediate, but rather reflects the entire cumulative emission of Hg. Motivated by a reconstructed history of atmospheric Hg through time (Streets et al., 2017), we subject our model to a 4.5 times increase, following an initial spinup equilibration period of 10,000 years. The beginning of the anthropogenic period corresponds to about the year 1880 in reality, and the enhanced emission is continued for 220 years, corresponding to simulated year 2100, after which the Hg deposition rate abruptly declines to natural levels. The abrupt decrease is simpler than the reality could be, because recycled Hg fluxes from the land surface and from the ocean itself would fuel continued enhanced Hg deposition to the ocean for centuries and longer. However, our modeling scenario of abruptly terminating anthropogenic emissions allows us to determine the time constant of the oceanic recovery. We also simulate a "hangover" scenario in which an abrupt cessation of human Hg emissions triggers a gradual slowdown of enhanced deposition, over an ocean overturning time scale of 1,000 years.

2.5 Method Limitations

The steady state assumption in the Hg solvers limits the ability of Hg-HAMOCC to explore detailed shallow-water interactions of turbulence, ventilation, and photochemistry, but the physics of the tracer advection code preclude much of that anyway. The model allows us to explore the interaction of the Hg chemistry and particle adsorption with the ocean circulation on long time scales.

A peculiarity of the surface ocean solver is that net sea surface fluxes of Hg are always balanced, by construction, exclusive of advective Hg fluxes. The PO_4 solver in HAMOCC incorporates the biological uptake kinetics into the iterative advective solver (Maier-Reimer, 1984), but the relationship of Hg degassing rates to the Hg concentration is nonlinear, and no attempt was made to replicate Ernst's example. Because Hg concentrations in the top box are determined by a balance of fluxes with the atmosphere, in places where surface divergence brings up Hg from below, the advective upwelling source is missed by Hg-HAMOCC, which will underestimate the Hg surface concentrations and degassing rates somewhat. To use the model to simulate a transient uptake of Hg by the ocean in response to a change in the surface rain rate, we can track the change in global ocean inventory of Hg with time, but the fluxes determined by the solver at the air-sea interface will balance to zero, defiant of the net fluxes that are filling the deep ocean with Hg. The top box of the model serves as a sort of boundary condition for Hg. This is similar to the treatment of O_2 in HAMOCC, for similar reasons.

Biogeosciences Discuss., https://doi.org/10.5194/bg-2018-117
Manuscript under review for journal Biogeosciences
Discussion started: 7 March 2018

3 Results

3.1 Reaction Kinetics and Pathways

The impact of the Hg cycle on fish and people occurs primarily through MMHg, which is a minor component of total Hg in the ocean. An implication is that any perturbation to the MMHg fraction of total Hg could have a huge leveraging impact on fish and people, analogously to the way that a change in ocean pH could have a huge impact on atmospheric pCO_2.

The fast reaction kinetics in the ocean Hg cycle imply that local variations in reaction kinetics will drive MMHg variability, rather than large-scale advection of MMHg by ocean circulation. By construction in the model, and apparently to a large extent in the real ocean, the reactions that produce and consume MMHg in the dark are biologically mediated and self-balancing, resulting in a nearly uniform proportion of MMHg of total Hg in the deep ocean. However, the MMHg production rate varies in the real ocean, with enhanced production in low-oxygen environments (Chakraborty et al., 2016). Rates also depend on the quality of dissolved organic matter (terrestrial vs. marine: (Schartup et al., 2015)), and can be shut down by complexation with dissolved sulfide in anoxic environments (Lamborg et al., 2008). Future changes in climate may affect MMHg production in the ocean, such as decreasing oxygen solubility in a warmer ocean (Blackwell et al., 2014;Eagles-Smith et al., 2018).

A suggestion of the scope for changing MMHg is illustrated using the model in Figure 7. The top panel shows the relative change in MMHg concentration at 250 meters water depth from enhancing MMHg production in low-oxygen waters (increasing by a factor of 1+exp(-O2/50 micromolar)). The largest changes are up to a factor of 4, in the low-oxygen, high surface productivity equatorial Pacific. This increase is comparable to the enhanced MMHg concentrations resulting from 200 years of a four-times enhanced deposition of Hg to the surface ocean (our simple anthropocene), shown at the same 250 meters water depth in Figure 7b.

3.2 Particle Sinking versus the Overturning Circulation

There are two competing mechanisms for Hg invasion into the deep ocean: advection by the overturning circulation and the flux of Hg adsorbed on sinking particles. We use our model to explore the interaction of these pathways. There are two end-member cases to consider; one with particles dominating the distribution and transport of Hg, and the other with circulation dominating. In the particle-dominating case, the steady state constraint is that the vertical flux of Hg has to be depth-invariant; the fluxes have to balance at any depth level. The particle-flux dominating end member condition can be achieved in Hg-HAMOCC by disabling the advection of the Hg tracers (Figure 8, orange line). The result is that, in the steady state, Hg concentrations rise with depth in the ocean, to compensate for the decrease in sinking POC flux. A smaller POC sinking flux will have to carry a higher Hg density in order to sustain the required depth-uniform Hg flux, and the higher adsorbed Hg density requires a higher Hg concentration in the water column.

The other end-member case comes much closer to the observed distribution of Hg in the deep ocean. When circulation dominates and particle transport of Hg is disabled, the Hg concentrations maintained in the surface ocean (by balancing

evasion against deposition) are imposed on the deep ocean, resulting in a nearly uniform distribution of Hg throughout the ocean (Figure 8, blue line). There are some regional variations in Hg, but they are not systematic, as compared to the clear Pacific – Atlantic differences exhibited by nutrient-type elements (concentrated in the Pacific) versus by strongly scavenged elements like Al (concentrated in the Atlantic, where deposition is more intense).

The balance between advection versus sinking particles affects the uptake of anthropogenic Hg by the ocean. Profiles of total Hg changes from pre-anthropogenic to present-day, after 230 years of enhanced Hg deposition, are shown in Figure 9. If particles are neglected or sink so slowly as to be negligible in the Hg cycle, there is a sharp surface spike in Hg concentrations in the analog present day, due to increased deposition. An increasing importance of particle transport tends to moderate a surface ocean spike, while transferring much of the anthropogenic Hg load to a subsurface maximum corresponding to the location of POC degradation in the thermocline.

Particulate Hg transport to depth is required in order to simulate a subsurface maximum in Hg concentration, as observed in the present-day real ocean. In the steady state, with no anthropogenic enhanced deposition, a somewhat slower Hg sinking flux would still generate a subsurface maximum, but it is harder to have a subsurface maximum at the end of a period of enhanced Hg deposition, as today.

Figure 10 shows the total uptake of anthropogenic Hg in that deposition period, as a function of the Hg particle sinking velocity. Particle transport has only a minor impact on the global rate of Hg uptake during the anthropocene stage, but strong particle transport has the effect of sequestering the anthropogenic Hg deeper in the ocean (Figure 9), where it is retained somewhat longer than in models with less particle transport.

The model when forced with an instantaneous end to anthropogenic emissions predicts that the ocean will continue degassing Hg for 1000 years. When this prediction is turned around, to impose a condition that the Hg deposition rate declines over 1000 years after our 230-year "anthropocene" ending in the present day, the duration of the anthropogenic Hg load on the oceans increases to several thousand years. The top panel in Figure 10 shows the result of a sudden (unrealistic) return to pre-anthropogenic Hg deposition rates, while in the bottom panel the rate of Hg deposition decreases exponentially from anthropogenic values with a time scale of 1000 years (a "hangover" scenario.

3.3 Isotopic Fractionation

Isotopic fractionations in the Hg cycle can be expressed (or not) in the isotopic signatures of the Hg species, depending on the pathways of chemical transformation. Results are shown in Figures 11-15. The isotopic composition of oceanic Hg is set at the sea surface. A guiding principle in understanding these results is that in the steady state the isotopic degassing flux, a combination of Hg(0) and DMHg degassing fluxes, has to balance isotopically the input by Hg(2+) rain, which is 0.4‰ in δ^{202} and 0.05‰ in Δ^{199}. Some fractionation effect that we impose in the model pulls the isotopic composition of either Hg(0) or DMHg away from these values, and the other has to go the opposite way to compensate. Then the values of the other species, MMHg, and Hg(2+), are pulled in various ways by their connections with the two gases.

Biogeosciences Discuss., https://doi.org/10.5194/bg-2018-117
Manuscript under review for journal Biogeosciences
Discussion started: 7 March 2018

It has been observed that there is a large difference in the D199 values of MMHg versus Hg(2+) in ocean surface waters (MMHG results from fish: (Blum et al., 2013)). We were forced to modify the web of reactions and kinetics proposed by (Semeniuk and Dastoor, 2017), in particular the formulation of the interreaction between Hg(2+) and MMHg. In (Semeniuk and Dastoor, 2017), MMHg is demethylated to Hg(2+) directly. When configured in this way, the Hg cycle was unable to fractionate MMHg without Hg(2+) following along, because of this reaction. The isotopic composition of total Hg throughout the entire ocean picked up this fractionation signature. A solution is to alter the reaction web so that demethylation produces an intermediary Hg(0), which homogenizes with the rest of the Hg(0) pool before fueling a necessary next step to Hg(2+), which takes place at a faster rate constant than in (Semeniuk and Dastoor, 2017), to compensate for the greater overall traffic of Hg(0) going to Hg(2+). This pathway is consistent with the photochemical mechanism for Hg reaction, which involves accepting an electron to form an intermediary Hg(1).

3.3.1 Gas Evasion Fractionations

Beginning with gas exchange fractionation in Figure 11a, a fractionation associated with evasion of Hg(0) to the atmosphere, with faster rates for the lighter isotope as always in the model, leaves a dissolved Hg(0) pool that is residually heavy, about +0.1‰. The Hg(0) evasion flux has an isotopic signature of 0.1 – 0.4 = -0.3‰, which must be balanced by the loss of Hg with a positive isotopic composition, by evasion of DMHg and burial of deep water Hg(2+) adsorbed onto particles.

Fractionation in DMHg degassing (Figure 11b) is similar in that the δ^{202} of the degassing fractionating species (DMHg) goes residually positive. Because DMHg is not returned to the Hg pool as quickly in the model as Hg(0), the isotopic deviation in DMHg does not pass to the other pools, which remain near 0 ‰. Fractionating during evaporation of both gases simultaneously (Figure 11c) shows that the effects of each fractionation are additive.

3.3.2 Reaction Fractionations

The expression (or not) of a fractionation in a reaction pathway in the Hg cycle depends on the web of reactions between the species and the mass balance constraints. Fractionating the reduction step from Hg(2+) to Hg(0) (Figure 11d) has only a slight impact on the isotopic signatures of any of the species, because there is more Hg(0) produced from MMHg than from Hg(2+). In constrast, fractionating the MMHg -> Hg(0) step (Figure 11e) causes MMHg to get lighter, and to pass an isotopically light signature to Hg(0). Hg(2+) gets residually heavier. This couples to DMHg, which also remains heavier than the other species. The steady state is found where the isotopically negative evasion flux of Hg(0) is balanced by the flux of heavy Hg-P from the deep ocean. As another example, fractionating MMHg -> Hg(0), in Figure 11f, makes Hg(0) isotopically light, and MMHg residually heavy, which pulls DMHg toward a heavy signature to balance the degassing fluxes.

Depth profiles of Hg(2+) δ^{202} values are shown in Figure 12. A fractionation in Hg adsorption onto particles tends to leave behind a residually heavy Hg throughout the entire ocean, in response to the isotopically negative Hg burial flux. The surface is held closer than the deep to the 0‰ signature of Hg(2+) atmospheric deposition. The deep ocean Hg is actually

isotopically heavier than the surface, counter to the intuition that adsorbing and removing isotopically light Hg from the surface ocean should leave the surface ocean residually heavy. Fractionation in MMHg production leaves Hg(2+) in the deep ocean residually heavy, while fractionation in MMHg reduction results in Hg(2+) that is isotopically light. In both cases, the isotopic composition near the sea surface is again held near 0‰.

Maps of regional heterogeneity in the distribution of δ^{202} Hg(2+), at the sea surface and at 3 km depth, are shown in Figure 13. Most of the fractionation mechanisms are sensitive to primary productivity and particle export, as can be seen in a vivid plume of isotopic anomaly in the equatorial Pacific. However, the impact of productivity on particle fractionation is of opposite sign to that of MMHg reduction and gas evasion of Hg(0). The regional heterogeneity is reduced somewhat when all of the fractionation mechanisms are combined, because of this cancellation. Of the fractionation mechanisms, dark reactions involving MMHg production or destruction are the only ones that generate a deep Atlantic / Pacific contrast in δ^{202} Hg(2+).

3.3.3 Mass Independent Fractionations

Mass-independent fractionations imposed on photochemical reactions (Figure 11i-k, Figures 14-15) behave in the same mass-balancing way as the MDF results presented above. Of the two cases, a fractionation in demethylation (MMHg -> Hg(0)) has the strongest expression, and the response of the isotopic signatures of the aqueous Hg species is similar to the MDF impacts shown in Figure 11e. However, an imposed fractionation in photoreduction of Hg(2+) to Hg(0) is not expressed in the isotopic abundances, similarly to the MDF case in Figure 11f. A map of the sea surface Δ^{199}MMHg at the sea surface (Figure 15) reflects the intensity of photochemical reaction in the model.

4 Conclusions

We have embedded a model of Hg chemistry and dynamics into the HAMOCC off-line ocean tracer advection model, including for the first time treatment of isotopic fractionation in the ocean Hg cycle. The efficiency of the model makes it possible to do numerous sensitivity experiments, which is useful for developing intuition about this complex system.

The model demonstrates that the Hg cycle in the ocean is closer to a purely advective end member than to a system in which transport on sinking particles dominates, because the latter predicts an increase in Hg concentrations with depth, as the flux of sinking particles from the surface declines. A series of sensitivity runs with different Hg-P sinking velocities shows that the observed present-day subsurface maximum in [Hg(2+)] is a product of Hg sinking. Given the 4.5-times enhanced Hg deposition flux since about 1880 (Streets et al., 2017), if there were no Hg sinking and subsurface release on particles, the highest Hg concentrations would be at the sea surface today. Anthropogenic Hg sinking on particles does not have a strong impact on the net uptake rate of anthropogenic Hg by the ocean. But if the enhanced rates of Hg deposition were suddenly to return to natural levels, a model with strong Hg sinking takes longer to shed its anthropogenic Hg burden. Since oceanic Hg

evasion will be recycled to redeposition, the ocean system seems poised to buffer the environmental Hg concentration for thousands of years.

Isotopic variations in Hg can be used to constrain Hg cycling, especially powerfully because of the multiple "dimensions" of fractionation, with mass dependent fractionation that most processes might contribute to, and mass-independent fractionations that can only happen in photochemical reactions. The Hg cycle in the ocean is complex enough that a model is required, to predict the "expression" of isotopic fractionations in processes on the isotopic signatures of Hg species in the ocean, and the distribution of variations in those signatures. There is wide variation in the expression of isotope fractionation effects in the isotopic composition of Hg standing stocks. The most dramatic Hg isotope signature in the ocean is probably the Δ^{199} of MMHg that accumulates in fish ((Blum et al., 2013)); our model is able to replicate the magnitude of that isotopic shift, and the distinction between MMHg and Hg(2+), using the measured fractionation factor from Bergquist and Blum (2007). Other predicted regional variations in δ^{202}Hg(2+) include a correlation with the rate of primary productivity in the surface ocean for some mechanisms, but that much of this correlation cancels out in the sum of all processes, because the signs of the impact differ among the processes. Another spatial signature to look for is the gradient in the δ^{202}Hg(2+) of the deep Atlantic vs. Pacific, which results in the model mostly from dark reactions creating and destroying MMHg.

References

Amos, H. M., Jacob, D. J., Streets, D. G., and Sunderland, E. M.: Legacy impacts of all-time anthropogenic emissions on the global mercury cycle, Global Biogeochemical Cycles, 27, 410-421, 10.1002/gbc.20040, 2013.

Anderson, R. F., Cheng, H., Edwards, R. L., Fleisher, M. Q., Hayes, C. T., Huang, K. F., Kadko, D., Lam, P. J., Landing, W. M., Lao, Y., Lu, Y., Measures, C. I., Moran, S. B., Morton, P. L., Ohnemus, D. C., Robinson, L. F., and Shelley, R. U.: How well can we quantify dust deposition to the ocean?, Philosophical Transactions of the Royal Society a-Mathematical Physical and Engineering Sciences, 374, 10.1098/rsta.2015.0285, 2016.

Archer, D. E., Eby, M., Brovkin, V., Ridgewell, A. J., Cao, L., Mikolajewicz, U., Caldeira, K., Matsueda, H., Munhoven, G., Montenegro, A., and Tokos, K.: Atmospheric lifetime of fossil fuel carbon dioxide, Ann. Reviews Earth Planet Sci., 37, 117-134, 2009.

Balogh, S. J., Tsui, M. T. K., Blum, J. D., Matsuyama, A., Woerndle, G. E., Yano, S., and Tada, A.: Tracking the Fate of Mercury in the Fish and Bottom Sediments of Minamata Bay, Japan, Using Stable Mercury Isotopes, Environmental Science & Technology, 49, 5399-5406, 10.1021/acs.est.5b00631, 2015.

Bergquist, B. A., and Blum, J. D.: Mass-dependent and -independent fractionation of Hg isotopes by photoreduction in aquatic systems, Science, 318, 417-420, 10.1126/science.1148050, 2007.

Bergquist, R. A., and Blum, J. D.: The Odds and Evens of Mercury Isotopes: Applications of Mass-Dependent and Mass-Independent Isotope Fractionation, Elements, 5, 353-357, 10.2113/gselements.5.6.353, 2009.

Biswas, A., Blum, J. D., and Keeler, G. J.: Mercury storage in surface soils in a central Washington forest and estimated release during the 2001 Rex Creek Fire, Science of the Total Environment, 404, 129-138, 10.1016/j.scitotenv.2008.05.043, 2008.

Blackwell, B. D., Driscoll, C. T., Maxwell, J. A., and Holsen, T. M.: Changing climate alters inputs and pathways of mercury deposition to forested ecosystems, Biogeochemistry, 119, 215-228, 10.1007/s10533-014-9961-6, 2014.

Blum, J. D.: Mesmerized by mercury, Nature Chemistry, 5, 1066-1066, 10.1038/nchem.1803, 2013.

Blum, J. D., Popp, B. N., Drazen, J. C., Choy, C. A., and Johnson, M. W.: Methylmercury production below the mixed layer in the North Pacific Ocean, Nature Geoscience, 6, 879-884, 10.1038/ngeo1918, 2013.

Blum, J. D., Sherman, L. S., and Johnson, M. W.: Mercury Isotopes in Earth and Environmental Sciences, in: Annual Review of Earth and Planetary Sciences, Vol 42, edited by: Jeanloz, R., Annual Review of Earth and Planetary Sciences, 249-269, 2014.

Chakraborty, P., Mason, R. P., Jayachandran, S., Vudamala, K., Armoury, K., Sarkar, A., Chakraborty, S., Bardhan, P., and Naik, R.: Effects of bottom water oxygen concentrations on mercury distribution and speciation in sediments below the oxygen minimum zone of the Arabian Sea, Marine Chemistry, 186, 24-32, 10.1016/j.marchem.2016.07.005, 2016.

Chen, C. Y., Driscoll, C. T., Lambert, K. F., Mason, R. P., and Sunderland, E. M.: Connecting mercury science to policy: from sources to seafood, Reviews on Environmental Health, 31, 17-20, 10.1515/reveh-2015-0044, 2016.

Clarkson, T. W., and Magos, L.: The toxicology of mercury and its chemical compounds, Critical Reviews in Toxicology, 36, 609-662, 10.1080/10408440600845619, 2006.

Demers, J. D., Sherman, L. S., Blum, J. D., Marsik, F. J., and Dvonch, J. T.: Coupling atmospheric mercury isotope ratios and meteorology to identify sources of mercury impacting a coastal urban-industrial region near Pensacola, Florida, USA, Global Biogeochemical Cycles, 29, 1689-1705, 10.1002/2015gb005146, 2015.

Donovan, P. M., Blum, J. D., Demers, J. D., Gu, B. H., Brooks, S. C., and Peryam, J.: Identification of Multiple Mercury Sources to Stream Sediments near Oak Ridge, TN, USA, Environmental Science & Technology, 48, 3666-3674, 10.1021/es4046549, 2014.

Driscoll, C. T., Mason, R. P., Chan, H. M., Jacob, D. J., and Pirrone, N.: Mercury as a Global Pollutant: Sources, Pathways, and Effects, Environmental Science & Technology, 47, 4967-4983, 10.1021/es305071v, 2013.

Eagles-Smith, C. A., Silbergeld, E. K., Basu, N., Bustamante, P., Diaz-Barriga, F., Hopkins, W. A., Kidd, K. A., and Nyland, J. F.: Modulators of mercury risk to wildlife and humans in the context of rapid global change, Ambio, 47, 170-197, 10.1007/s13280-017-1011-x, 2018.

Fitzgerald, W. F., Lamborg, C. H., and Hammerschmidt, C. R.: Marine biogeochemical cycling of mercury, Chemical Reviews, 107, 641-662, 10.1021/cr050353m, 2007.

Gebbie, G., and Huybers, P.: The Mean Age of Ocean Waters Inferred from Radiocarbon Observations: Sensitivity to Surface Sources and Accounting for Mixing Histories, Journal of Physical Oceanography, 42, 291-305, 10.1175/jpo-d-11-043.1, 2012.

Han, S. H., Gill, G. A., Lehman, R. D., and Choe, K. Y.: Complexation of mercury by dissolved organic matter in surface waters of Galveston Bay, Texas, Marine Chemistry, 98, 156-166, 10.1016/j.marchem.2005.07.004, 2006.

Hollweg, T. A., Gilmour, C. C., and Mason, R. P.: Mercury and methylmercury cycling in sediments of the mid-Atlantic continental shelf and slope, Limnology and Oceanography, 55, 2703-2722, 10.4319/lo.2010.55.6.2703, 2010.

Horowitz, H. M., Jacob, D. J., Amos, H. M., Streets, D. G., and Sunderland, E. M.: Historical Mercury Releases from Commercial Products: Global Environmental Implications, Environmental Science & Technology, 48, 10242-10250, 10.1021/es501337j, 2014.

Jonsson, S., Mazrui, N. M., and Mason, R. P.: Dimethylmercury Formation Mediated by Inorganic and Organic Reduced Sulfur Surfaces, Scientific Reports, 6, 10.1038/srep27958, 2016.

Krabbenhoft, D. P., and Sunderland, E. M.: Global Change and Mercury, Science, 341, 1457-1458, 10.1126/science.1242838, 2013.

Kritee, K., Blum, J. D., Johnson, M. W., Bergquist, B. A., and Barkay, T.: Mercury stable isotope fractionation during reduction of Hg(II) to Hg(0) by mercury resistant microorganisms, Environmental Science & Technology, 41, 1889-1895, 10.1021/es062019t, 2007.

Kritee, K., Barkay, T., and Blum, J. D.: Mass dependent stable isotope fractionation of mercury during mer mediated microbial degradation of monomethylmercury, Geochimica Et Cosmochimica Acta, 73, 1285-1296, 10.1016/j.gca.2008.11.038, 2009.

Kwon, S. Y., Blum, J. D., Chirby, M. A., and Chesney, E. J.: Application of mercury isotopes for tracing trophic transfer and internal distribution of mercury in marine fish feeding experiments, Environmental Toxicology and Chemistry, 32, 2322-2330, 10.1002/etc.2313, 2013.

Kwon, S. Y., Blum, J. D., Chen, C. Y., Meattey, D. E., and Mason, R. P.: Mercury Isotope Study of Sources and Exposure Pathways of Methylmercury in Estuarine Food Webs in the Northeastern US, Environmental Science & Technology, 48, 10089-10097, 10.1021/es5020554, 2014.

Lamborg, C., Bowman, K., Hammerschmidt, C., Gilmour, C., Munson, K., Selin, N., and Tseng, C. M.: MERCURY in the Anthropocene Ocean, Oceanography, 27, 76-87, 10.5670/oceanog.2014.11, 2014.

Lamborg, C. H., Yigiterhan, O., Fitzgerald, W. F., Balcom, P. H., Hammerschmidt, C. R., and Murray, J.: Vertical distribution of mercury species at two sites in the Western Black Sea, Marine Chemistry, 111, 77-89, 10.1016/j.marchem.2007.01.011, 2008.

Lamborg, C. H., Hammerschmidt, C. R., and Bowman, K. L.: An examination of the role of particles in oceanic mercury cycling, Philosophical Transactions of the Royal Society a-Mathematical Physical and Engineering Sciences, 374, 10.1098/rsta.2015.0297, 2016.

Lehnherr, I., St Louis, V. L., Hintelmann, H., and Kirk, J. L.: Methylation of inorganic mercury in polar marine waters, Nature Geoscience, 4, 298-302, 10.1038/ngeo1134, 2011.

Lehnherr, I.: Methylmercury biogeochemistry: a review with special reference to Arctic aquatic ecosystems, Environmental Reviews, 22, 229-243, 10.1139/er-2013-0059, 2014.

Li, M. L., Sherman, L. S., Blum, J. D., Grandjean, P., Mikkelsen, B., Weihe, P., Sunderland, E. M., and Shine, J. P.: Assessing Sources of Human Methylmercury Exposure Using Stable Mercury Isotopes, Environmental Science & Technology, 48, 8800-8806, 10.1021/es500340r, 2014.

Maier-Reimer, E.: Towards a global ocean carbon model, Prog. Biometeorology, 3, 295-310, 1984.

Maier-Reimer, E., and Hasselmann, K.: Transport and storage of CO2 in the ocean - an inorganic ocean-circulation carbon cycle model, Climate Dynamics, 2, 63-90, 10.1007/bf01054491, 1987.

Maierreimer, E., Mikolajewicz, U., and Hasselmann, K.: MEAN CIRCULATION OF THE HAMBURG LSG OGCM AND ITS SENSITIVITY TO THE THERMOHALINE SURFACE FORCING, Journal of Physical Oceanography, 23, 731-757, 10.1175/1520-0485(1993)023<0731:mcothl>2.0.co;2, 1993.

Mason, R. P., Choi, A. L., Fitzgerald, W. F., Hammerschmidt, C. R., Lamborg, C. H., Soerensen, A. L., and Sunderland, E. M.: Mercury biogeochemical cycling in the ocean and policy implications, Environmental Research, 119, 101-117, 10.1016/j.envres.2012.03.013, 2012.

Munson, K. M., Lamborg, C. H., Swarr, G. J., and Saito, M. A.: Mercury species concentrations and fluxes in the Central Tropical Pacific Ocean, Global Biogeochemical Cycles, 29, 656-676, 10.1002/2015gb005120, 2015.

Obrist, D., Kirk, J. L., Zhang, L., Sunderland, E. M., Jiskra, M., and Selin, N. E.: A review of global environmental mercury processes in response to human and natural perturbations: Changes of emissions, climate, and land use, Ambio, 47, 116-140, 10.1007/s13280-017-1004-9, 2018.

Ortiz, V. L., Mason, R. P., and Ward, J. E.: An examination of the factors influencing mercury and methylmercury particulate distributions, methylation and demethylation rates in laboratory-generated marine snow, Marine Chemistry, 177, 753-762, 10.1016/j.marchem.2015.07.006, 2015.

Ray, E. A., Moore, F. L., Elkins, J. W., Rosenlof, K. H., Laube, J. C., Rockmann, T., Marsh, D. R., and Andrews, A. E.: Quantification of the SF6 lifetime based on mesospheric loss measured in the stratospheric polar vortex, Journal of Geophysical Research-Atmospheres, 122, 4626-4638, 10.1002/2016jd026198, 2017.

Rose, C. H., Ghosh, S., Blum, J. D., and Bergquist, B. A.: Effects of ultraviolet radiation on mercury isotope fractionation during photo-reduction for inorganic and organic mercury species, Chemical Geology, 405, 102-111, 10.1016/j.chemgeo.2015.02.025, 2015.

Schartup, A. T., Mason, R. P., Balcom, P. H., Hollweg, T. A., and Chen, C. Y.: Methylmercury Production in Estuarine Sediments: Role of Organic Matter, Environmental Science & Technology, 47, 695-700, 10.1021/es302566w, 2013.

Schartup, A. T., Ndu, U., Balcom, P. H., Mason, R. P., and Sunderland, E. M.: Contrasting Effects of Marine and Terrestrially Derived Dissolved Organic Matter on Mercury Speciation and Bioavailability in Seawater, Environmental Science & Technology, 49, 5965-5972, 10.1021/es506274x, 2015.

Schartup, A. T., Qureshi, A., Dassuncao, C., Thackray, C. P., Harding, G., and Sunderland, E. M.: A Model for Methylmercury Uptake and Trophic Transfer by Marine Plankton, Environmental Science & Technology, 52, 654-662, 10.1021/acs.est.7b03821, 2018.

Schuster, P. F., Schaefer, K. M., Aiken, G. R., Antweiler, R. C., Dewild, J. F., Gryziec, J. D., Gusmeroli, A., Hugelius, G., Jafarov, E., Krabbenhoft, D. P., Liu, L., Herman-Mercer, N., Mu, C., Roth, D. A., Schaefer, T., Striegl, R. G., Wickland, K. P., and Zhang, T.: Permafrost Stores a Globally Significant Amount of Mercury, Geophysical Research Letters, 45, 10.1002/2017GL075571, 2018.

Semeniuk, K., and Dastoor, A.: Development of a global ocean mercury model with a methylation cycle: Outstanding issues, Global Biogeochemical Cycles, 31, 400-433, 10.1002/2016gb005452, 2017.

Sherman, L. S., Blum, J. D., Franzblau, A., and Basu, N.: New Insight into Biomarkers of Human Mercury Exposure Using Naturally Occurring Mercury Stable Isotopes, Environmental Science & Technology, 47, 3403-3409, 10.1021/es305250z, 2013.

Sherman, L. S., Blum, J. D., Basu, N., Rajaee, M., Evers, D. C., Buck, D. G., Petrlik, J., and DiGangi, J.: Assessment of mercury exposure among small-scale gold miners using mercury stable isotopes, Environmental Research, 137, 226-234, 10.1016/j.envres.2014.12.021, 2015.

Smith-Downey, N. V., Sunderland, E. M., and Jacob, D. J.: Anthropogenic impacts on global storage and emissions of mercury from terrestrial soils: Insights from a new global model, Journal of Geophysical Research-Biogeosciences, 115, 10.1029/2009jg001124, 2010.

Streets, D. G., Devane, M. K., Lu, Z. F., Bond, T. C., Sunderland, E. M., and Jacob, D. J.: All-Time Releases of Mercury to the Atmosphere from Human Activities, Environmental Science & Technology, 45, 10485-10491, 10.1021/es202765m, 2011.

Streets, D. G., Horowitz, H. M., Jacob, D., Lu, Z. F., Levin, L., ter Schure, A. F. H., and Sunderland, E. M.: Total Mercury Released to the Environment by Human Activities, Environmental Science & Technology, 51, 5969-5977, 10.1021/acs.est.7b00451, 2017.

Wiederhold, J. G., Cramer, C. J., Daniel, K., Infante, I., Bourdon, B., and Kretzschmar, R.: Equilibrium Mercury Isotope Fractionation between Dissolved Hg(II) Species and Thiol-Bound Hg, Environmental Science & Technology, 44, 4191-4197, 10.1021/es100205t, 2010.

Zhang, Y. X., Jaegle, L., Thompson, L., and Streets, D. G.: Six centuries of changing oceanic mercury, Global Biogeochemical Cycles, 28, 1251-1261, 10.1002/2014gb004939, 2014.

Biogeosciences Discuss., https://doi.org/10.5194/bg-2018-117
Manuscript under review for journal Biogeosciences
Discussion started: 7 March 2018

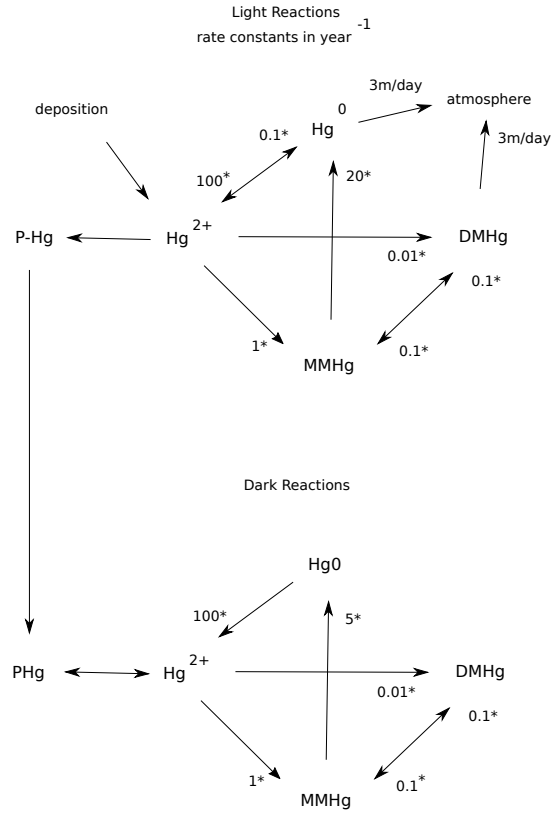

Figure 1. Schematic of the reaction web for Hg speciation in the model. Starred numbers by the arrows show rate constants, relative to the rate of MMHg production (which is derived at each grid cell by the degradation rate of POC at that point).

Biogeosciences Discuss., https://doi.org/10.5194/bg-2018-117
Manuscript under review for journal Biogeosciences
Discussion started: 7 March 2018

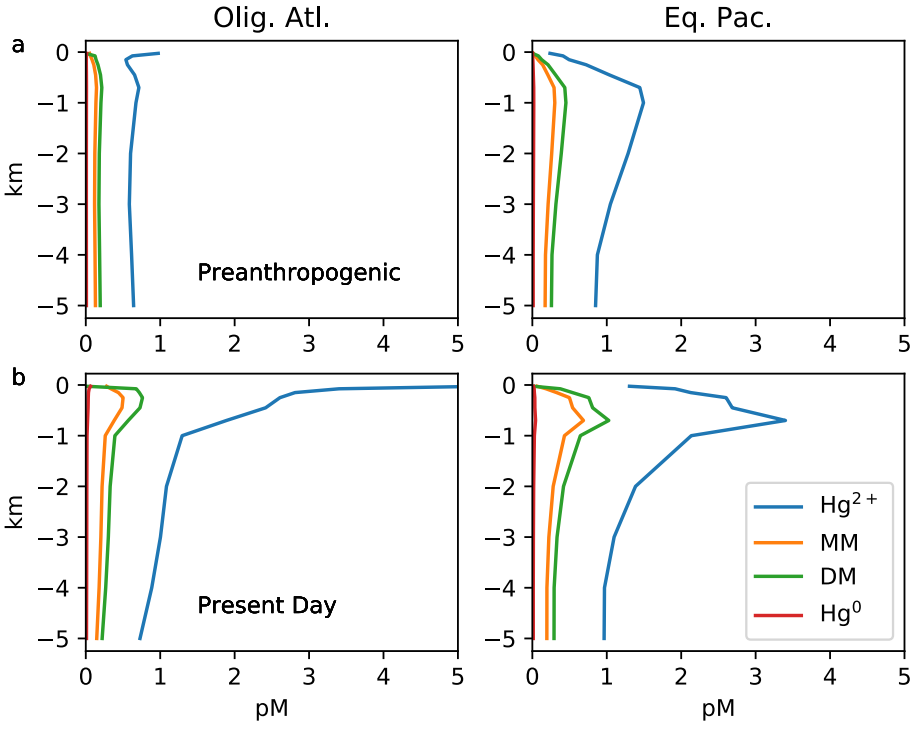

Figure 2. Depth profiles of the speciation of Hg in the model from locations shown on Figure 3.

Biogeosciences Discuss., https://doi.org/10.5194/bg-2018-117
Manuscript under review for journal Biogeosciences
Discussion started: 7 March 2018

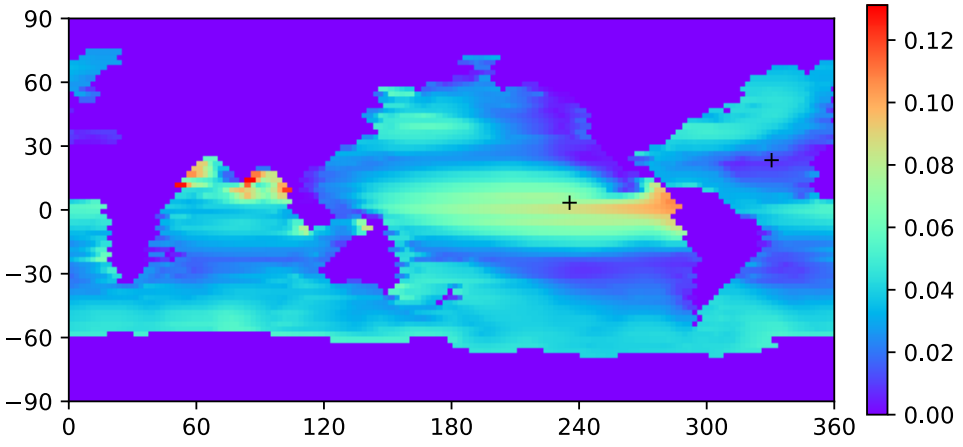

Figure 3. A map of the bound fraction of Hg(2+) when the K_d value is $1 \cdot 10^4$, resulting in approximately 5% bound Hg(2+) in surface waters on average, with higher values in high-POC productive regions.

Biogeosciences Discuss., https://doi.org/10.5194/bg-2018-117
Manuscript under review for journal Biogeosciences
Discussion started: 7 March 2018

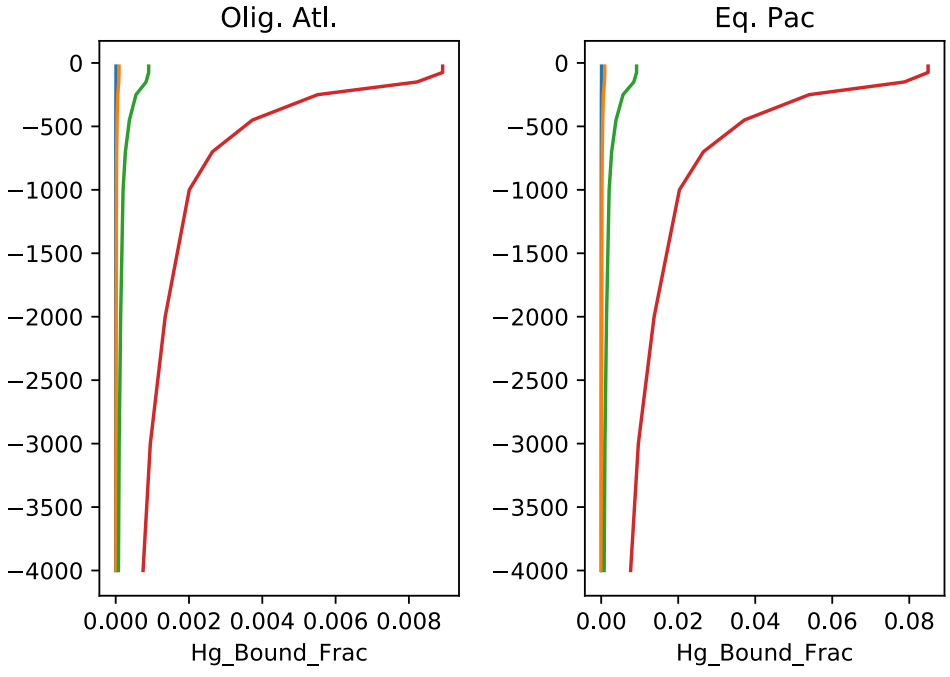

Figure 4. Depth profiles of the bound fraction of Hg(2+) from the same locations as in Figure 2, as a function of the K_d value. A value of $1 \cdot 10^4$ (red lines) is used in the rest of the model simulations.

Biogeosciences Discuss., https://doi.org/10.5194/bg-2018-117
Manuscript under review for journal Biogeosciences
Discussion started: 7 March 2018

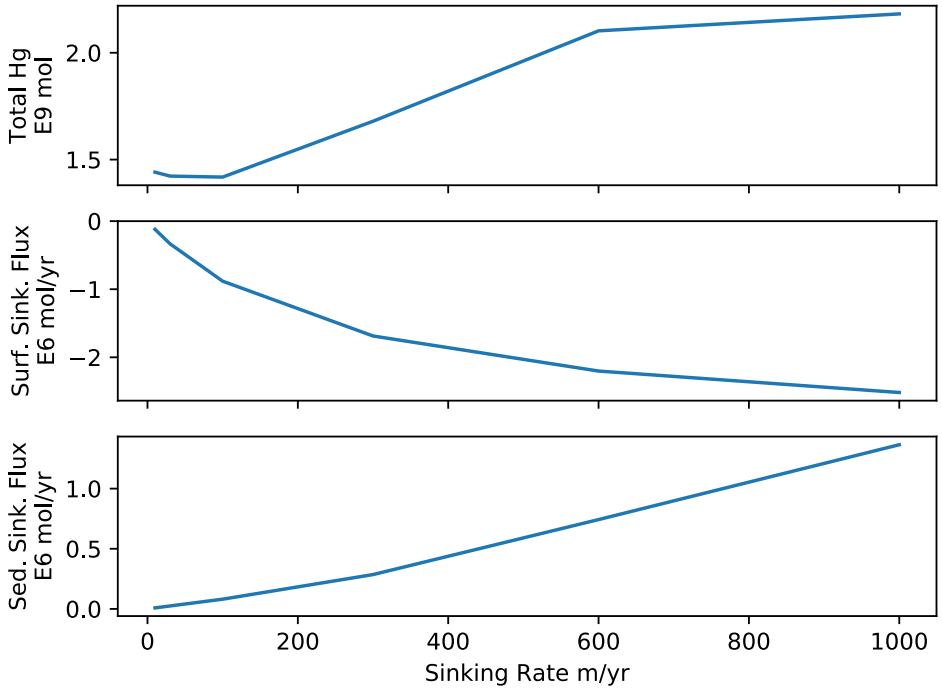

Figure 5. Model fluxes as a function of Hg(2+) sinking velocity imposed in the model. A default value of 400 m / year is used in the rest of the simulations.

Biogeosciences Discuss., https://doi.org/10.5194/bg-2018-117
Manuscript under review for journal Biogeosciences
Discussion started: 7 March 2018

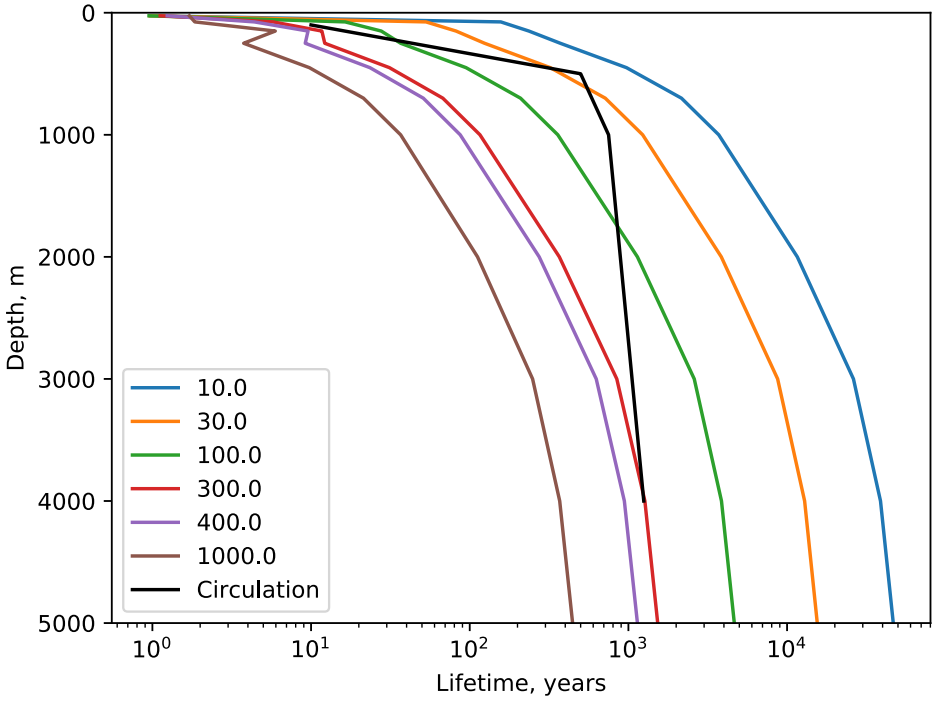

Figure 6. Profiles of the turnover time of Hg(2+) with respect to transiting through the system on sinking particles, as a function of the sinking velocity in the legend, in m/yr. The black line is the water age since exposure to the atmosphere derived from the ^{14}C distribution (Gebbie and Huybers, 2012).

Biogeosciences Discuss., https://doi.org/10.5194/bg-2018-117
Manuscript under review for journal Biogeosciences
Discussion started: 7 March 2018

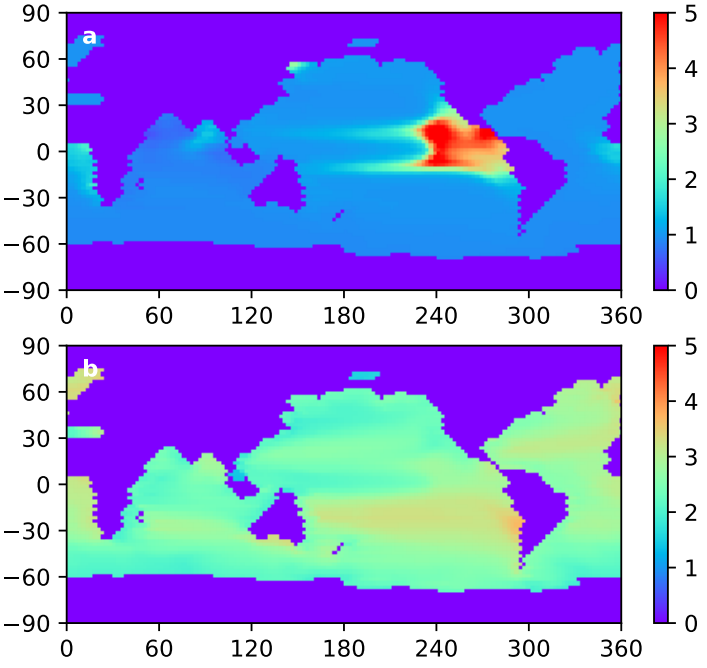

Figure 7. Maps of the ratio of the concentration of MMHg at 250 meters water depth, relative to a base case. A) Result of enhanced MMHg production in low-oxygen waters, relative to the case of no low-oxygen enhancement. B) Result of 200 years of quadrupled Hg(2+) deposition to the sea surface.

Biogeosciences Discuss., https://doi.org/10.5194/bg-2018-117
Manuscript under review for journal Biogeosciences
Discussion started: 7 March 2018

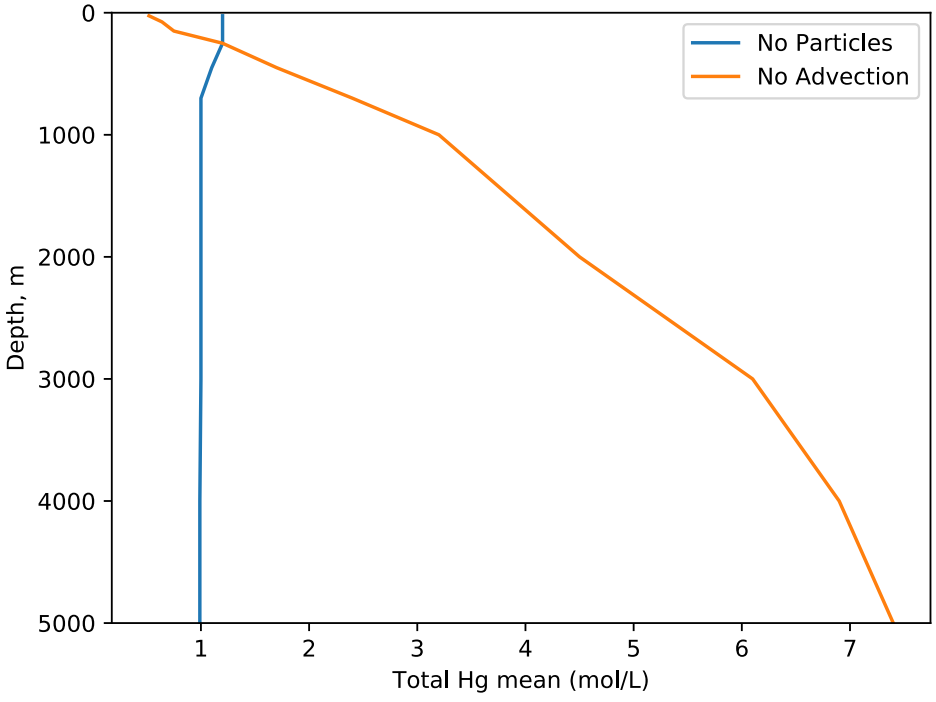

Figure 8. Profiles of mean Hg concentration as a function of depth in the ocean, in equilibrium, for the end-member cases of no particles (blue line), and no advection (orange line).

Biogeosciences Discuss., https://doi.org/10.5194/bg-2018-117
Manuscript under review for journal Biogeosciences
Discussion started: 7 March 2018

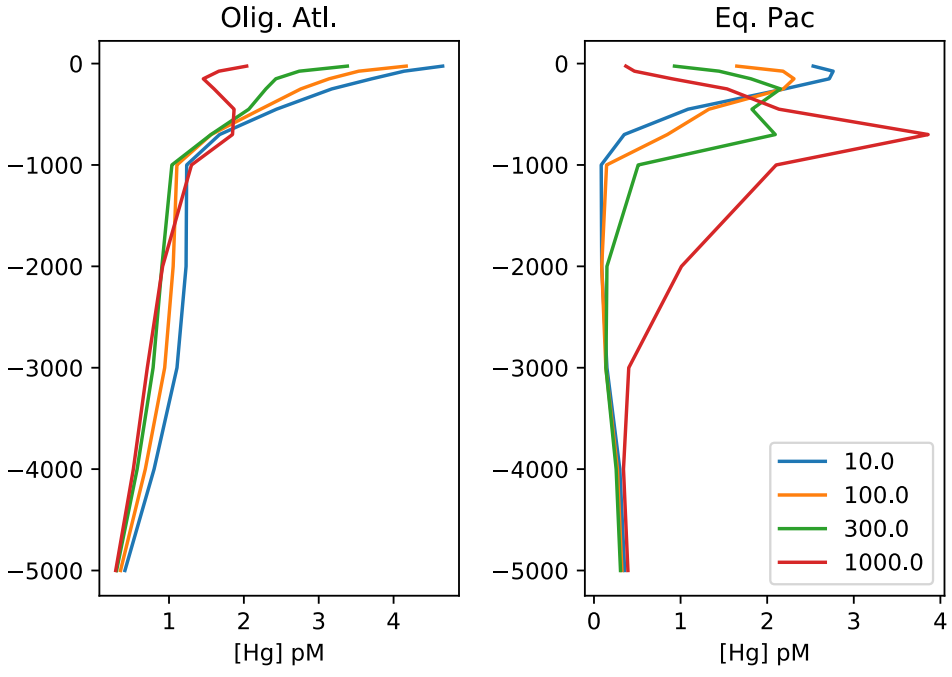

Figure 9

Figure 9. Profiles of the change in total Hg concentration following 230 years of enhanced anthropogenic Hg(2+) deposition, for different values of the Hg-particle sinking velocity in m/yr.

Biogeosciences Discuss., https://doi.org/10.5194/bg-2018-117
Manuscript under review for journal Biogeosciences
Discussion started: 7 March 2018

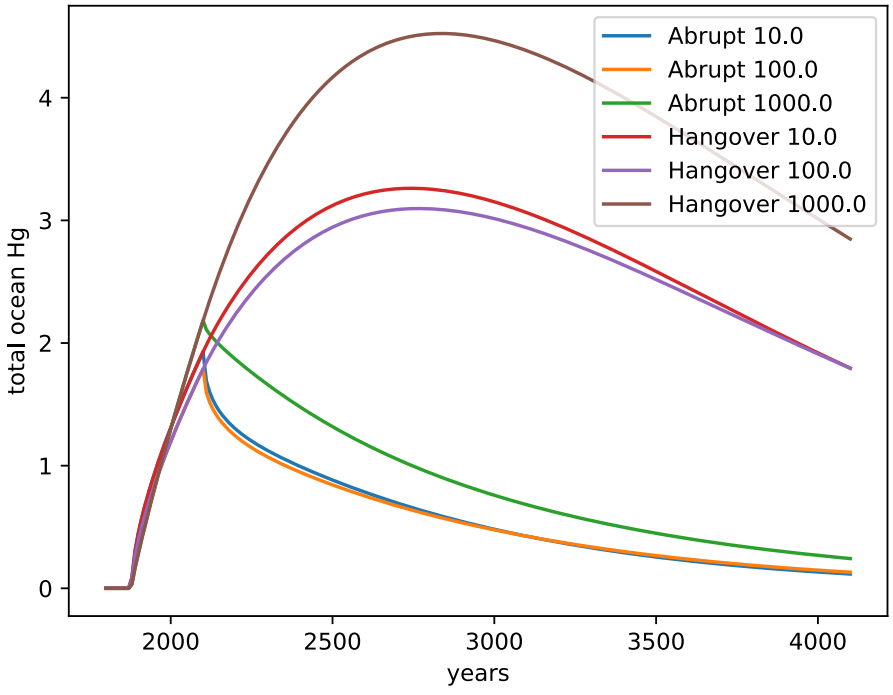

Figure 10. Time series of the ocean load of Hg in response to 230 years of enhanced Hg(2+) deposition, followed by immediate return to natural deposition rates, or 1000-year wind-down in anthropogenic deposition due to recycling from the ocean.

Biogeosciences Discuss., https://doi.org/10.5194/bg-2018-117
Manuscript under review for journal Biogeosciences
Discussion started: 7 March 2018

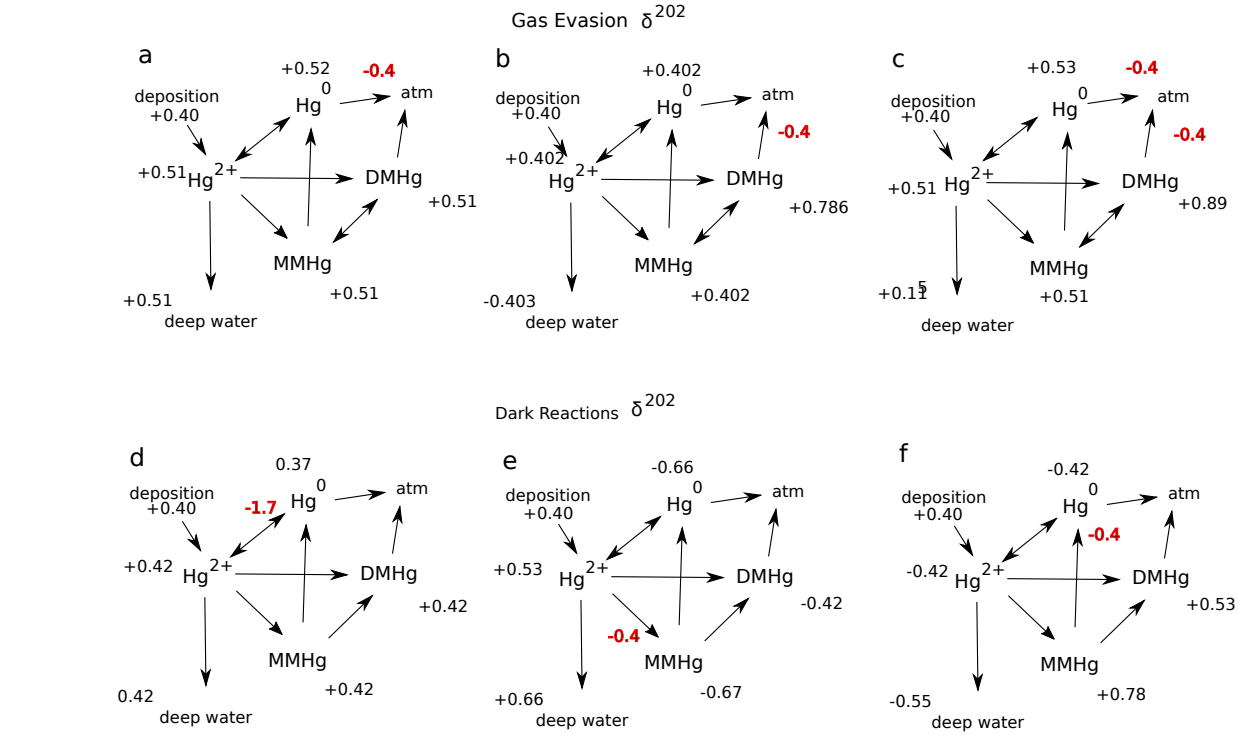

Biogeosciences Discuss., https://doi.org/10.5194/bg-2018-117
Manuscript under review for journal Biogeosciences
Discussion started: 7 March 2018

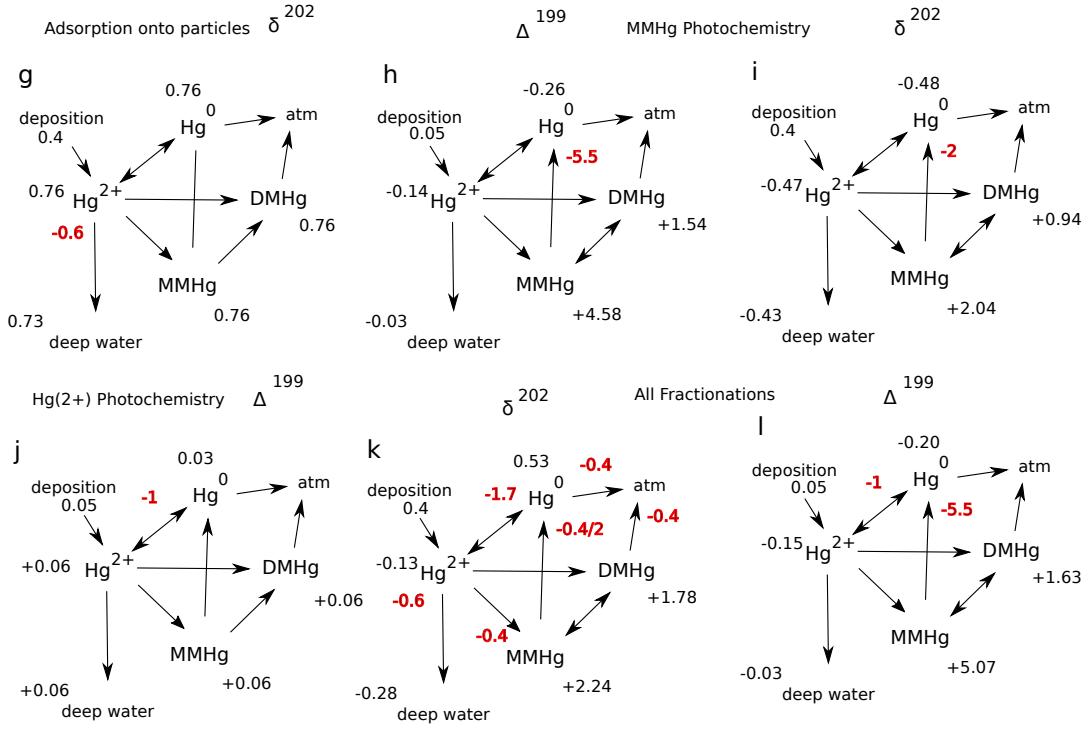

Figure 11. Schematic of the expression of isotopic fractions on the isotopic signatures of the Hg species in the model. Fractionations are shown in red, expressed as per mille between 202 and 198. Resulting average δ^{202} values for each species are in black. A) Mass dependent fractionation applied to Hg(0) evasion (Wiederhold et al., 2010). B) applied to DM Hg degassing (assuming the same fractionation as for Hg(0) evasion). C) Both gas evasion fractionations applied simultaneously. The results in C are the sum of those in A and B. D) Fractionation is applied in the reduction of Hg(2+) to form Hg(0) (Kritee et al., 2007); E) in the methylation of Hg(2+) to form MMHg (Kritee et al., 2009); F) in demethylation / reduction of MMHg to form Hg(0). G) shows the impact of fractionation in particle adsorption. H) shows photochemical demethylation Δ^{199} MIF mass independent fractionation results, while (I) is the effect on δ^{202} from that process , using the ratio of Δ^{199} to δ^{202} that results and (i) Hg(2+) reduction.

Biogeosciences Discuss., https://doi.org/10.5194/bg-2018-117
Manuscript under review for journal Biogeosciences
Discussion started: 7 March 2018

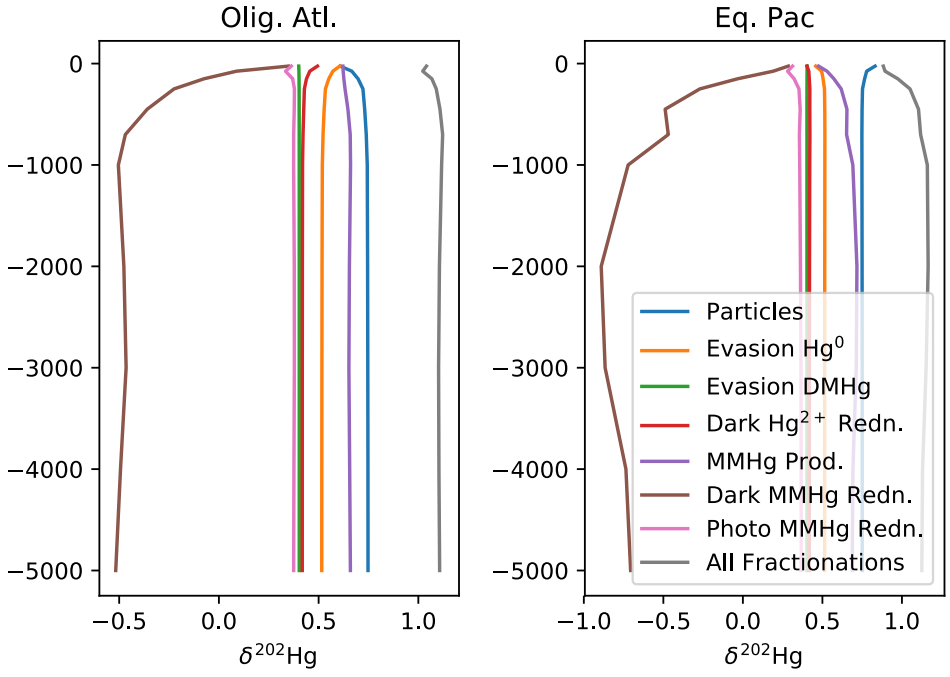

Figure 12. Profiles of δ^{202}Hg(2+) for different fractionation scenarios.

Biogeosciences Discuss., https://doi.org/10.5194/bg-2018-117
Manuscript under review for journal Biogeosciences
Discussion started: 7 March 2018

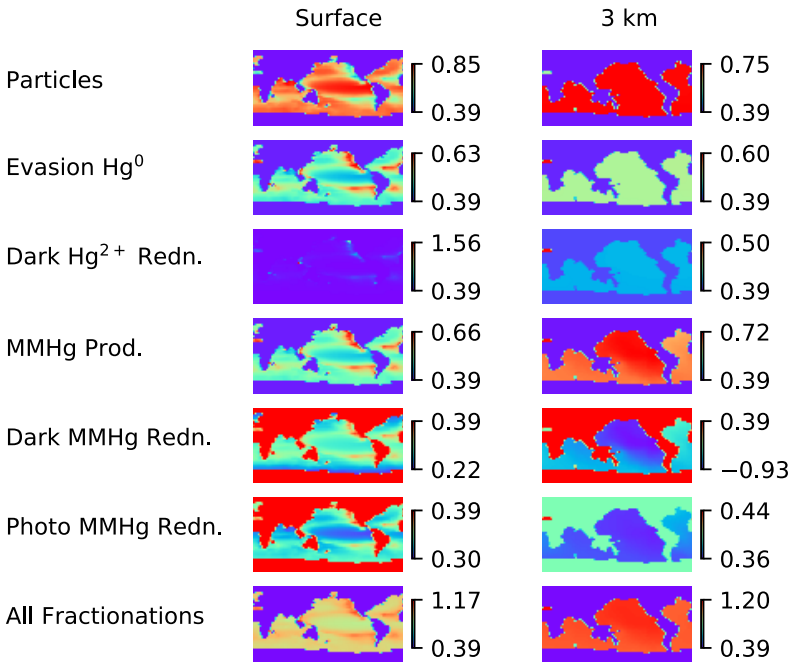

Figure 13. Maps of δ^{202}Hg(2+) at the sea surface (left) and at 3 km depth (right) for different fractionation scenarios.

Biogeosciences Discuss., https://doi.org/10.5194/bg-2018-117
Manuscript under review for journal Biogeosciences
Discussion started: 7 March 2018

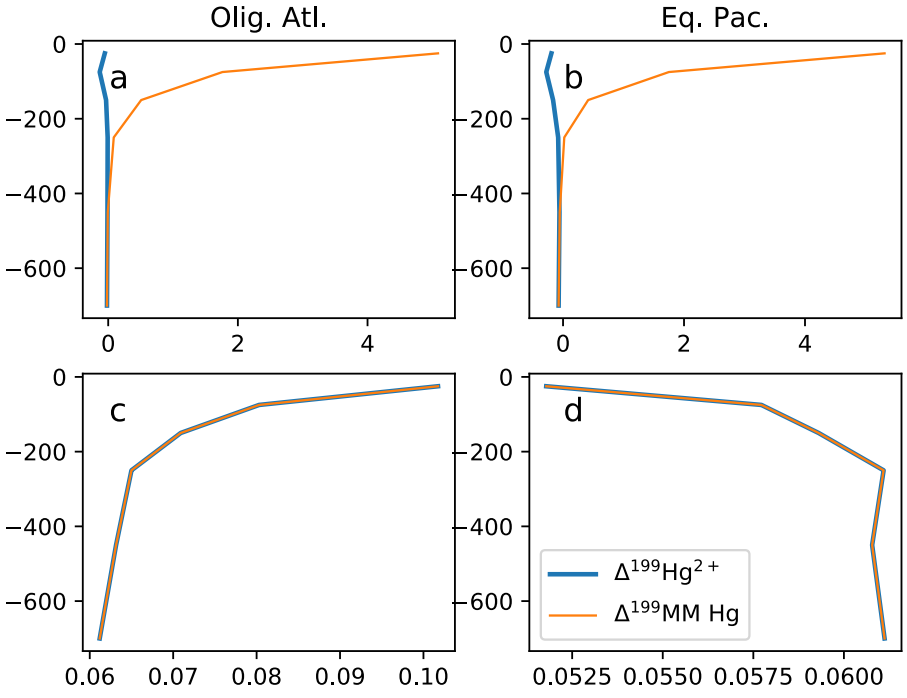

Figure 14. Profiles of Δ^{199} of MMHg for the two different photochemical MIF fractionation scenarios.

Biogeosciences Discuss., https://doi.org/10.5194/bg-2018-117
Manuscript under review for journal Biogeosciences
Discussion started: 7 March 2018

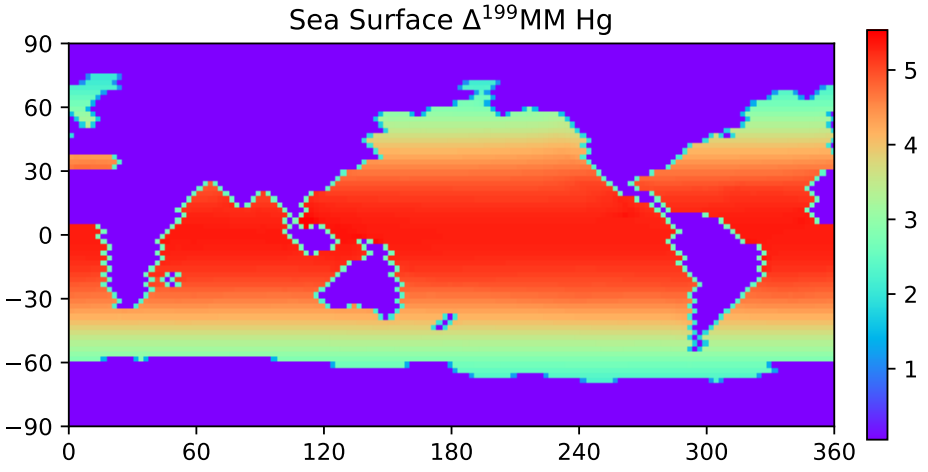

Figure 15. A map of sea surface Δ^{199} of MMHg showing a latitudinal dependence due to the intensity of sunlight driving photochemical reactions.